LAWRENCE
LIVERMORE
NATIONAL
LABORATORY

LLNL-JRNL-734772

Metal Alloy Inertial Confinement Fusion Capsules Created by Electrodeposition

C. A. Horwood, M. Stadermann, T. L. Bunn

July 14, 2017

Fusion Science and Technology

Disclaimer

Metal Alloy ICF Capsules Created by Electrodeposition

Corie Horwood, Michael Stadermann and Thomas L. Bunn

Lawrence Livermore National Laboratory, P.O. Box 808, Livermore, CA 94550

Abstract

Electrochemical deposition is an attractive alternative to physical vapor deposition and micromachining to produce metal capsules for inertial confinement fusion (ICF). Electrochemical deposition (also referred to as electrodeposition or plating) is expected to produce full density metal capsules without seams or inclusions of unwanted atomic constituents, the current shortcomings of micromachine and physical vapor deposition, respectively.

Here we discuss new cathode designs that allow for the rapid electrodeposition of gold and copper alloys on spherical mandrels by making transient contact with the constantly moving spheres. Electrodeposition of pure gold, copper, platinum, and alloys of gold/copper and gold/silver are demonstrated, with non-porous coatings of > 40 μm achieved in only a few hours of plating. The surface roughness of the spheres after electrodeposition is comparable to the starting mandrel, and the coatings appear to be fully dense with no inclusions.

A detailed understanding of the electrodeposition conditions that result in different alloy compositions and plating rates will allow for the electrodeposition of graded alloys on spheres in the near future. This report on the electrodeposition of metals on spherical mandrels is an important first step towards the fabrication of graded density metal capsules for ICF experiments at the National Ignition Facility (NIF).

Keywords: electrodeposition, plating, alloys

I. Introduction

The hydrogen-isotope fuel for inertial confinement fusion (ICF) experiments on the National Ignition Facility (NIF) is generally contained inside a spherical plastic, diamond or beryllium capsule. This low atomic number (Z) capsule is categorized as a single pusher ablator or single shell target.[1] In an indirect drive configuration, 192 lasers heat a cylindrical gold hohlraum to generate X-rays incident on the capsule causing it to reach very high radial density and temperature under compression and undergo thermonuclear burn.

A double shell is another indirect drive target approach that couples hohlraum-generated X-ray energy more efficiently into the outer shell ablator and may lead to ignition. Double shell targets are concentric, spherical capsules where the inner shell is composed of high-Z elements such as copper (Cu), silver (Ag) or gold (Au) (or an alloy) and the outer shell is a low-Z metal such as Be or Al. Between the two shells is a layer of low density plastic or metal foam.[2] During ICF, the imploding outer shell impacts the high-Z inner shell filled with high-density room-temperature or cyrogenic H-isotope fuel. The inelastic collision of the outer shell with the inner shell magnifies the transfer of energy to the inner shell leading to a volume ignition rather than the point ignition of single pusher shell. The physics advantages of a complex double shell include the ability to: carry-out ICF implosions at room temperature; reduce fuel pre-heat because of high inner shell opacity; eliminate requirement for multiple shocks that necessitate laser pulse shaping and timing; and reduce the deleterious effects of laser plasma interactions on laser drive uniformity[3] by delivering impulsive energy to the outer shell on a shorter time scale. Some of the research and experiments carried out to model, develop and evaluate double shell targets are chronicled in the ICF literature.[4–13]

Our paper is focused on the production of the smooth, freestanding, mid- to high-Z metal inner capsule needed to assemble a double shell target. There have been at least three methods attempted to produce metal capsules including magnetron sputtering, electro- and electroless-deposition and chemical vapor deposition.[14,15] The critical aspects for each of these methods include (1) the microsphere mandrel must possess outstanding sphericity and surface smoothness, it must be resistant to scratching and cracking during deposition and ideally it should be readily removed following the coating process, (2) the microspheres must not stick to each other and must be in continuous random motion during the deposition and (3) the coatings must be dense, smooth and uniformly thick. Typical tolerance requirements for these capsules include radii from 100 to 300-μm, shell thicknesses from 10 to 60 μm, wall thickness nonuniformity less than 1%, sphericity of mandrel and coating less than 1% of radius, surface roughness less than 10-nm RMS and leak tight to hydrogen to over 200 atmospheres. The extreme smoothness and uniformity requirements are necessary to prevent the growth of Rayleigh-Taylor instabilities during the implosion which could lead to shell break-up and experimental failure.

Electroplating generally involves attaching a cathodic lead to a conducting part and applying a reducing potential in an electrolytic solution containing ions of the element to be plated. This tethered approach is not practical for microspheres because even the smallest attachment leaves an unacceptable “scar.” Several groups in the past 40 years have developed electrochemical cell variations for depositing metals on small substrates. Each configuration has common features. For example, they force intermittent and random contact between the sphere and a polarized cathode. They also agitate, circulate, filter and heat the electrolyte. Mayer et al[16–18] were the first to metal coat glass microspheres by successive autocatalytic and

electrodeposition to produce laser-fusion targets. They produced high quality microspheres plated with metal such as Cu, Ni, Ni-Fe and Au using commercially available solutions. Their coating thicknesses ranged from 12 to 250-µm. Illige et al[19,20] also electroplated glass microspheres with gold and copper using vibrating cathode and tapered cathode cells which, they claim, reduced the substrate and coating surface damage sustained by repeated impact in the electrochemical apparatus described by Mayer.[17]

Two and a half decades later, the Jankowski group also pursued the development of free-standing pressure vessels for ICF targets. Their objective was to enhance coating strength by measuring Au-Cu alloy coating morphology, hardness and solid composition as a function of cell potential,[21] thermal aging[22] and Sn additives[23] when electrodeposited on flat substrates. This group demonstrated that grain size, and thus hardness, could be adjusted through current density and additive concentration in a pulse current set-up.

Recently, Brun[24] and Durut[25] have extended Jankowski's research on Au-Cu electrodeposition in cyanide solutions using an apparatus invented by Botrel.[26] They studied the influence of electrochemical parameters on the properties of deposited films and correlated the relative copper content in the coating to the applied cell potential. Au is the more readily deposited metal while Cu is deposited after the diffusion limiting current density of Au is attained, at a potential of -1.0 V vs. a silver/silver-chloride reference electrode. A rise in bath temperature increases the kinetics of the reduction reaction of both gold and copper and promotes the deposition of copper preferentially. This group also developed a phenomenological model to better understand the electrocrystallization mechanisms that explains the evolutions of the

composition and roughness during electrodeposition as cell potential is varied. This model motivated a new coating process based on ultrasonic-assisted electrodeposition.

Here, we describe a new cathode cage apparatus to electroplate untethered microspheres with Au, Cu and alloys of these metals. The method possesses several advantages that improve coating quality, while minimizing non-productive cathode surface area and isolating microspheres for independent metrology before and after electrodeposition. As described in the reviewed literature, this new apparatus maintains the rolling or intermittent contact point between microsphere and cathode. The electrodeposition was demonstrated on Cu and glow discharge polymer (GDP) spherical mandrels having diameters between 1.8-2 mm. A future requirement is to remove the plastic mandrel through a pinhole to fabricate a freestanding metal shell, where the pinhole will become the socket for a gas fill tube. Another key challenge of this work is to deposit thick Au-Cu alloy coatings with a wide range of composition (ideally 100 % Au to 100 % Cu), varying *in situ* electroplating conditions to achieve gradient composition layers. Complete understanding of how the alloy composition varies with plating potential, along with a precise determination of plating rate as a function of overpotential will allow for the deposition of linear gradient composition of Au-Cu for the inner shell of the ICF double shell target.

II. Experimental

II.A. Materials

Brass foils (0.13 mm thick) were obtained from Alfa Aesar, while copper microsphere mandrels (grade 200, 2 mm diameter) were purchased from New England Miniature Ball company. A VWR Symphony bath sonicator was used to agitate the solution during electroplating.

Electroplating solutions contained 210 mM CN^-, 7 mM Au^+ and/or 45 mM Cu^+, added as KCN (96 %, Beantown Chemicals), $KAu(CN)_2$ (99.99 %, Alfa Aesar) and CuCN (99 %, Acros Organics). Solutions were prepared using deionized water (EMD Millipore Milli-Q Integral 5 Ultrapure Water System) and were filtered with 0.2 μm Nalgene filters between uses. Prior to electroplating, foils and spheres were cleaned by sonicating sequentially in acetone (99.9 %, Sigma Aldrich), isopropanol (99.5 %, Alfa Aesar) and water, then dried with a lint-free cloth.

Copper bus bar wire (38 gauge) was purchased from MSC Industrial Supply Co. Additively manufactured parts were made using MircoFine Green resin from Proto Labs.

II.B. Electrochemistry

Electrochemical measurements, data acquisition and electroplating experiments were performed using a Solartron Modulab XM potentiostat (Ametek-Solartron) and Modulab ECS software. All experiments were performed using a three-electrode cell configuration, with a Pt foil counter electrode (anode) and a Ag/AgCl reference electrode. The working electrode (cathode) was a brass foil or copper microsphere (mandrel).

II.C. Characterization

The surfaces of Pt deposits were examined by an optical microscope (Nikon C-DSD115 microscope with a Nikon SM21000 lens apparatus) with PAXcam software. SEM images were obtained using a Phenom ProX microscope with an accelerating voltage of 10-20 kV and secondary electron detection. White light interferometry (Veeco WYKO TN9800) was used to measure the average surface roughness of the mandrels before and after plating. Energy-dispersive X-ray (EDX) spectroscopy was used for elemental analysis, with an accelerating voltage of 10 kV. Au/Cu alloy standards were obtained from NIST, and the EDX was calibrated prior to measuring electroplated samples. The thickness of the coatings on spheres were measured using a Keyence high-speed optical micrometer (LS-9000).

III. Results and Discussion

III.A. Electrodeposition of alloys: Gold/copper composition variation with applied potential

Linear sweep voltammetry (Figure 1) in a solution containing cyanide plus either Au or Cu ions (added as a potassium cyanide salt) allows for the approximate potential of deposition to be determined. Gold deposition begins around -0.9 V vs. Ag/AgCl, and becomes diffusion limited at -1.3 V (peak in green trace in Figure 1). At ca. -1.7 V, hydrogen evolution becomes the dominant reaction occurring at the working electrode (cathode). Copper deposition occurs at higher overpotential, ca. -1.2 V (purple dashed trace in Figure 1) with diffusion limitation occurring around -1.6 V.

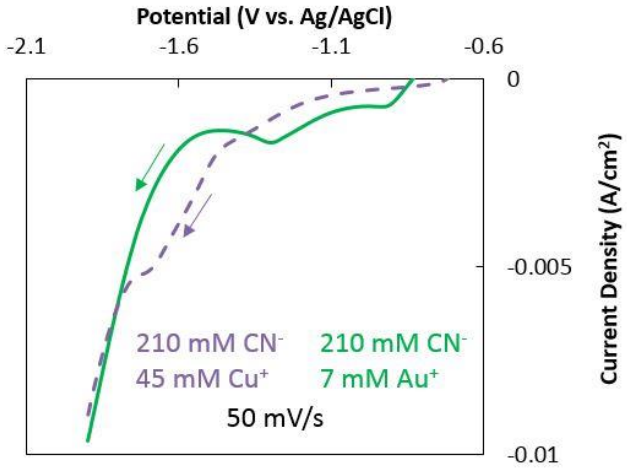

Figure 1. Linear sweep voltammetry in cyanide solution containing either Cu (purple dashed trace) or Au (green trace) cyanide. The potential was scanned from the open circuit potential (ca. -0.7—0.8 V) to -1.9 V vs. Ag/AgCl at 50 mV/s.

For potentials between open circuit (ca. -0.7 V) and ca. -1.2 V, only Au is expected to be plated. As the overpotential is increased (more negative potential), an alloy of Au and Cu will be plated, with the composition depending on the applied potential.

To determine the relationship between alloy composition and applied plating potential, several brass foils were plated in a cyanide-based plating bath containing 7 mM Au^{+} and 45 mM Cu^{+}. The potential was held at the desired voltage for 20 minutes to achieve coating thickness between 5 and 20-µm. Foils were plated in duplicate, and EDX spectra obtained at several points across each sample, were used to determine the Au and Cu composition in the solid coating. The EDX determined Au composition as a function of applied potential is shown in Figure 2 (a) below.

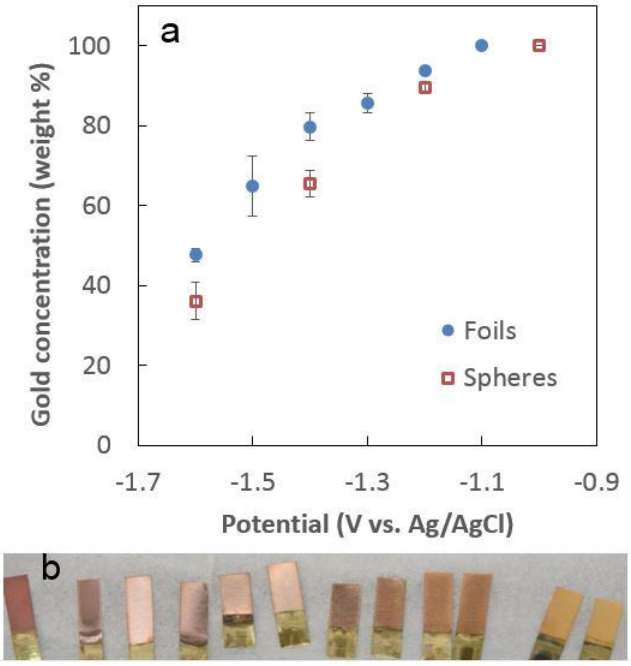

Figure 2. (a) EDX determined Au composition as a function of applied potential vs. Ag/AgCl for Au-Cu alloys plated on brass foils (blue solid points) and Cu microspheres (red hollow points). (b)

optical image of brass foils plated with Au-Cu alloys, with increasing Au composition from left to right.

Lower overpotentials had a significantly slower alloy coating rate than higher overpotentials (i.e. 0.1 µm/min at -1.1 V vs. 0.5 µm/min at -1.6 V). The electrodeposited alloy layers exhibited colors that varied with the applied potential (and alloy composition), as shown in Figure 2 (b).

III.B. Electrodeposition on untethered spheres: electrode designs

III.B.i. Ring cathode with rolling spheres

To achieve uniform, symmetrical coatings on spheres, the spheres must make random, transient contact with the cathode. Additionally, since lightweight hollow spheres will be used as mandrels, the cathode design must be able to accommodate the electroplating of mandrels that float (initial conditions) and sink (after > 10-µm metal coating). Additional desirable characteristics of the cathode include being inexpensive, easily replaceable, and the lowest possible surface area. The first cathode design tested here was comprised of two Cu ring cathodes, positioned above and below a doughnut-shaped, mesh enclosed cage (Figure 3 a). Microspheres were loaded into the two-piece cage, which was fabricated by additive manufacturing. The microspheres were propelled around the cage by viscous drag of the plating solution. A vortex was created by a magnetic stir-bar (positioned inside the doughnut-shaped cage) or by rotating the entire beaker while fixing the cage assembly.

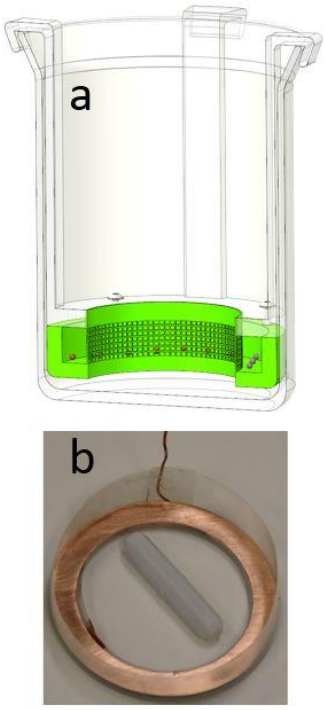

Figure 3: (a) Design for cage to contain ring cathode and rolling microspheres. A stir-bar in the center of the ring provides circular solution drag which causes the microspheres to roll around the ring. (b) Test prototype of copper ring cathode with plastic walls to contain microspheres.

While a simplified version of this cathode design (Figure 3b) was successful in electroplating CuAu alloys on microspheres, the design had several disadvantages. The large cathode surface area (relative to the surface area of the microspheres) results in significant depletion of Cu and Au metals from the plating solution. The plating solution must therefore be replaced or refreshed more frequently, thus increasing the cost of electroplating microspheres. Additionally, excessive deposition of Au and Cu on the rings results in Au-Cu build up on the rings, which resulted in undesirable surface roughness. After coatings of 10 µm, the buildup caused the microspheres to temporarily stick in groves that formed on the ring. This resulted in non-

uniform electroplating of the microspheres, and is thus a distinct disadvantage of this cathode design.

III.B.ii. Wire cage cathode

We have recently filed a patent application[27] for a new electroplating design, where microspheres (initially 2 mm in diameter) are contained within a cathode cage having dimensions ~ 3 mm x 5 mm. The frame of the cage is made by additive manufacturing using MicroFine Green (Figure 4). The frame consists of a ladder-like structure, with six parallel plates which make up the top and bottom for five separate cages. The plates have six 150 µm holes, arranged in a hexagonal pattern 1.5 mm from the plate center. Copper wires (100 µm diameter) are threaded through the six holes (with each wire making one pass down and up the entire cage frame) to create the vertical cage walls. The loose ends of the wires are bundled together at the top of the cage frame, where they are connected as the working electrode to the potentiostat.

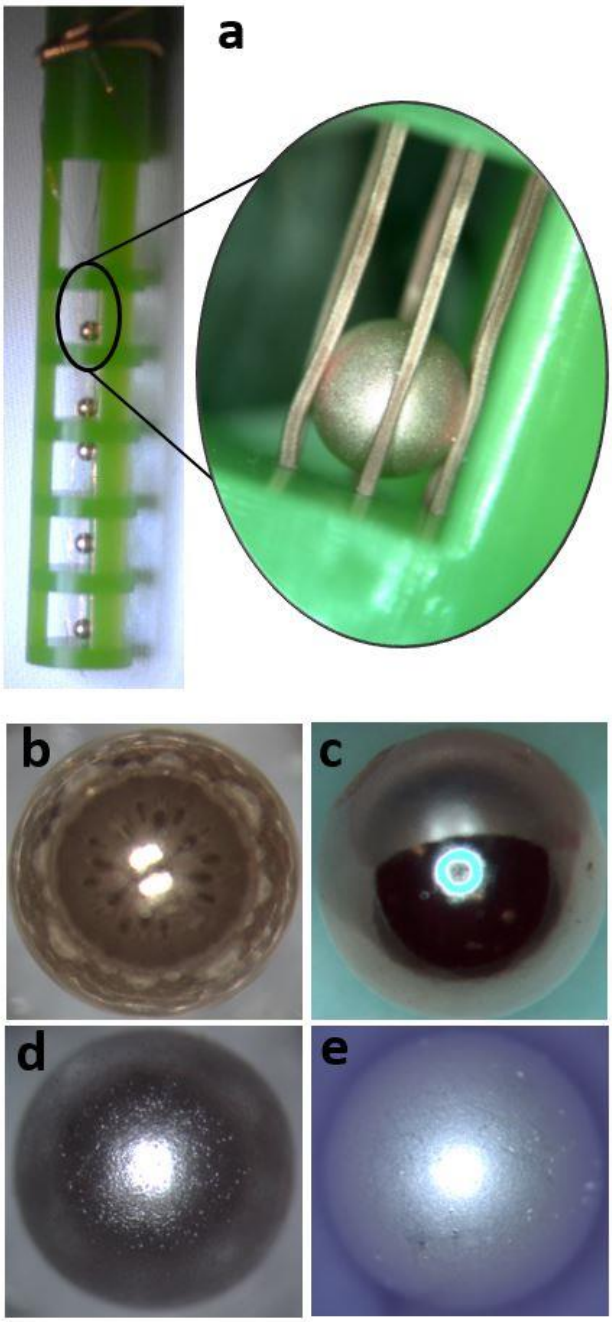

Figure 4: Image of (a) additive manufactured cage threaded with six 100 µm Cu wires (cathodes) containing five 2 mm diameter Cu microspheres which are separated by horizontal plates, before and (inset) after plating with Au-Cu. Optical microscope images of 2 mm diameter copper

mandrels electroplated with 20-40 µm thick coatings of (b) Au, (c) Cu, (d) platinum and (e) Ag-Au alloy.

The counter electrode was a perforated titanium foil rolled into a cylindrical shape. Platinum (platinum black) was electrodeposited to create the high surface area anode. The wire cage cathode frame was inserted into the center of the cylindrical counter electrode, which provides a uniform field around each microsphere inside the cage. Alternatively, a platinum or titanium wire could be wound around the outside of the frame of the cage, provided it does not contact the copper cathode wires. A silver/silver chloride reference electrode was placed ~ 1-cm from the two-electrode assembly during electrodeposition.[27]

The major advantages of this design are that the wire cage does not trap hydrogen bubbles formed at higher overpotentials and the buildup of Au and Cu on the cathode wires does not interfere with the motion of the spheres. Additionally, the relatively low cathode wire surface area (relative to microsphere surface area) results in less depletion of Au and Cu from the plating solution, which in turn results in more compact Au-Cu plating due to reduced diffusion limitations. The ~ 100 µm wires are also less likely to shield the microspheres from the solution mixing caused by stirring or sonication.

III.C. Gold/copper composition for untethered microspheres

The Au/Cu composition of several spheres electroplated using the wire cage design were evaluated by EDX. While the Cu composition fraction increased with increasing overpotential, as expected, the Au-Cu compositions at any given potential were not the same as those found for

Au-Cu deposits on Cu foils. As shown in Figure 2 (red hollow points), Au-Cu deposited on spheres was more Cu-rich when compared to alloy deposits on foils at the same potential.

The variation in Au-Cu composition between spheres and foils is thought to be caused by the nature of the contact between the untethered spheres and the cathode wires, or the movement of the spheres which alters the convection/diffusion of reactants to the microsphere. Further investigation using electrochemical impedance spectroscopy will help us better understand this phenomenon.

Nevertheless, the Au composition of the Au-Cu alloy can be varied from 100 to 35 % by changing the deposition potential from -1.0 V to -1.6 V. Further investigation into the effect of Au and Cu concentration in the plating solution, and extending the alloy composition range to include more copper is currently underway.

III.D. Surface finish and effect of sonication

The microsphere is moved around the wire cage by ultrasonic agitation. When the plating experiment is not performed in an ultrasonic cleaning bath, the microsphere is at rest in the wire cage, and will eventually stick and become welded to one or more of the wires. This results in a faster rate of plating and dendritic or rough deposits (Figure 5a). The improved surface finish with sonication was previously reported by CEA,[25] and confirmed here (Figure 5b).

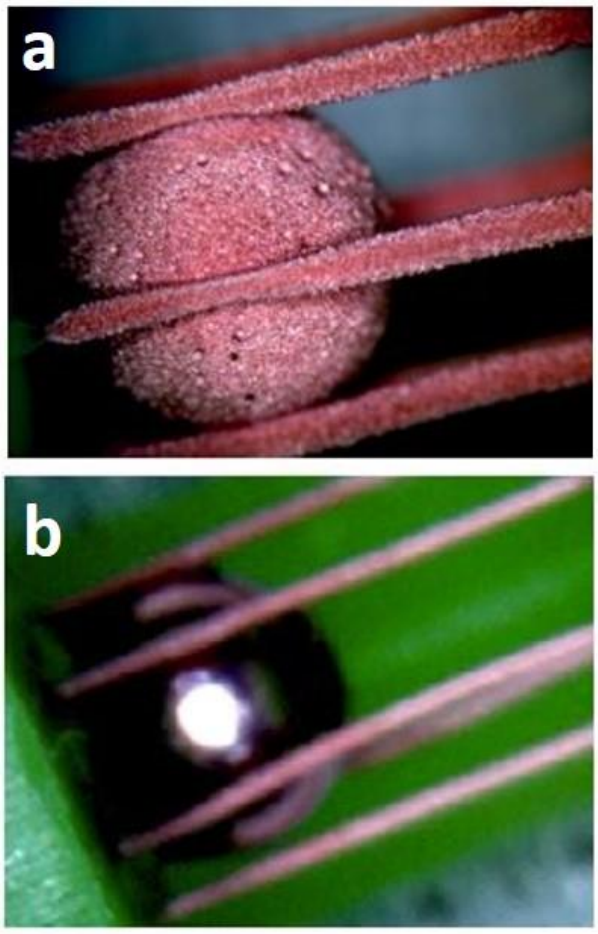

Figure 5. The effect of sonication on the surface finish of microspheres electroplated using the wire cage cathode design. (a) rough dendritic coatings obtained without sonication and (b) markedly smoother coatings obtained when a bath sonicator was used.

Scanning electron micrograph (SEM) images of AuCu alloys coated on copper mandrels show high uniformity of the coating across the entire mandrel surface (Figure 6, a & b). The surface features are ca. 5 µm in diameter and are present across the entire sample surface (Figure 6c). Occasionally, larger features of ca. 20 µm are found (i.e. the lower right corner of Figure 6b). These are thought to be caused by bumps on the Cu mandrels or inclusions of dislodged metal

(which is occasionally observed in the plating bath) which grow in diameter as the plated thickness increases (Figure 6e).

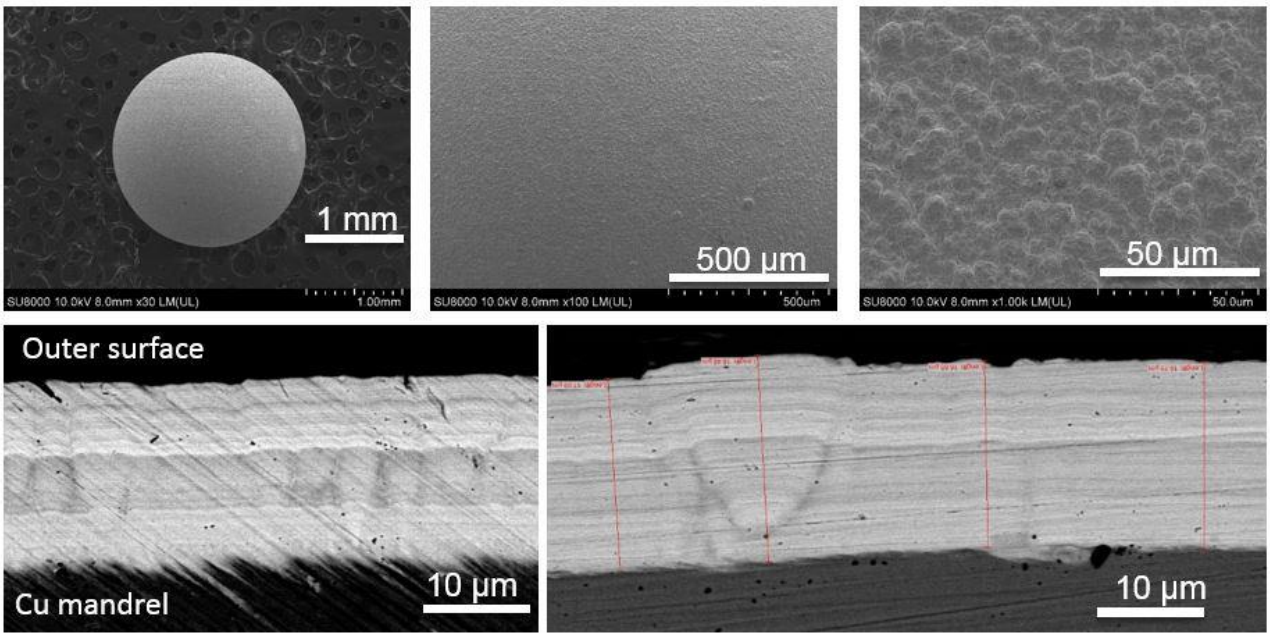

Figure 6. SEM images of a Cu mandrel (~ 2 mm diameter) electroplated with ~ 20 µm AuCu alloy. Electroplating was performed for 155 minutes at -1.2 V vs. Ag/AgCl at 70 ^{o}C, using a wire cage cathode, 7 mM Au^{+}, 45 mM Cu^{+}, 210 mM CN^{-}, using a bath sonicator.

Cross-sectional SEM images reveal striations in the coating, which are present throughout the entire coating. These are small variations (ca. 5-10 %) in the Au and Cu content of the alloy. While the cause of changing alloy composition during plating is currently unknown, there are several variables (i.e. temperature, magnitude of sonication) in the plating experiment that are prone to drifting/changing through the experiment.

WYKO white light interferometry was used to determine the surface roughness of the Cu mandrels before electroplating, and the resulting surface roughness after plating. The mandrels had a surface roughness of ca. 150 nm RMS (Figure 7a and d), while the surface roughness of Au-Cu coatings between 20-40 µm thick decreased (Figure 7b and e).

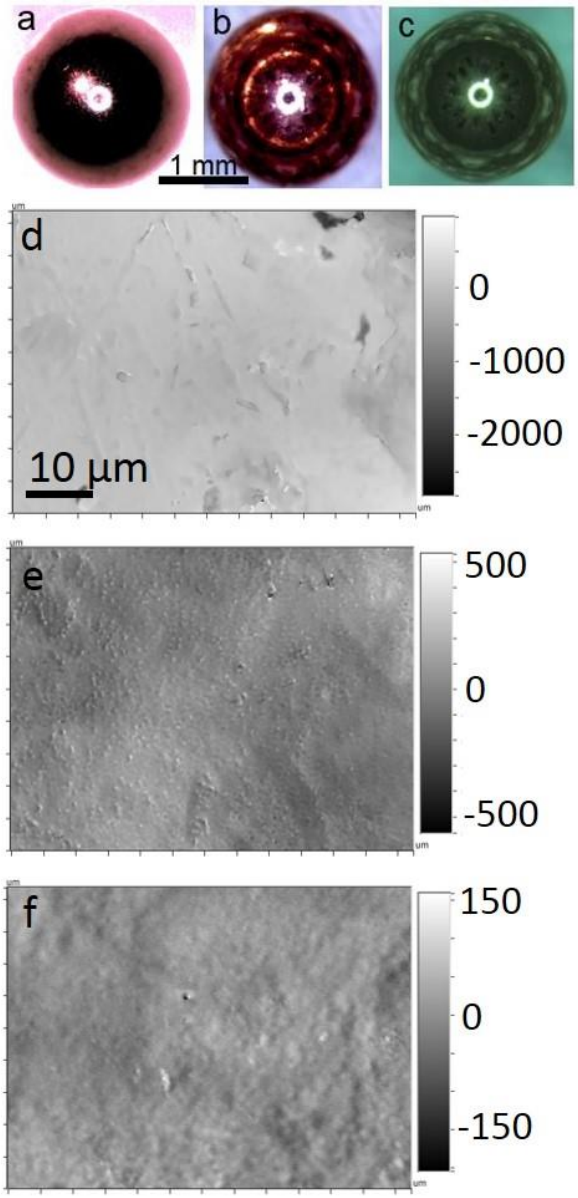

Figure 7. Optical microscope images of (a) a Cu microsphere mandrel before plating and (b) after plating ~ 20 µm of Cu-Au alloy and (c) ~ 17 µm of gold plated on a GDP mandrel. 1 mm scale bar applies to all

optical images. WYKO surface maps of (d) a Cu mandrel before plating (Ra = 150 nm) and (e) after plating with Cu-Au as described above (Ra = 60 nm), and (f) gold plated on GDP (Ra = 19 nm). 10 μm scale bar applies to all WYKO images, and individual height scales are indicated in nm.

As the surface finish after electroplating was typically found to be as good or better than that of the starting Cu mandrel, mandrels with lower surface roughness were used to evaluate the quality of the electroplating. GDP mandrels (1.8 μm diameter) were sputter coated with Au (100 nm) to provide a conductive strike layer (after sputter coating, RMS = 10 nm) followed by electroplating with Au (Figure 7c) using a commercially available gold plating bath (BDT-510, Enthone Inc). The resulting Au shell was found to have a surface roughness of ca. 19 nm RMS when an approximate thickness of 17 μm was deposited on the surface (Figure 7f).

III.E. Alloys and metals electroplated on microspheres

We have used the microsphere wire cage described to coat 2 mm diameter copper mandrels with a variety of metals and alloys, as shown in Figure 4 (b-e). While the plating rate varies with the metal or alloy being plated, we achieved 20-40 μm thick coatings of Au, Cu, Pt, and alloys of Au-Ag and Au-Cu in 1-6 hours.

IV. Conclusion

We have demonstrated the electrodeposition of metals (Au, Cu, and Pt) and alloys (Au-Cu, Au-Ag) on untethered, 2 mm diameter microsphere mandrels. Using the cathode wire cage described here, spheres can be plated with tens of micrometers of metal or alloy in short time periods, typically a couple of hours. The plating rate and alloy composition varies with applied potential, and compositions from 100 % Au to 35 % Au (65 % Cu) have been achieved by changing the deposition overpotential.

Ultrasonication causes the microspheres to move around the wire cage with random motion, which results in good thickness uniformity and surface finish. The average surface roughness after spherical mandrels were plated with ~ 20 μm was similar or better than the surface roughness of the mandrel before plating. Gold electrodeposited to a thickness of 17 μm on a GDP mandrel resulted in an average surface roughness of 19 nm RMS. This is a small roughness increase relative to the GDP mandrel surface (Ra = 10 nm).

The wire cage described here will enable the fabrication of graded alloy microspherical capsules by electrodeposition. The ability to control alloy composition with potential, and the rapid deposition of non-porous, adherent and smooth coatings on untethered microspheres makes electrodeposition a promising approach for capsule fabrication for ICF experiments for the NIF.

V. Acknowledgement

This work was performed under the auspices of the U.S. Department of Energy by Lawrence Livermore National Laboratory under Contract DE-AC52-07NA27344.

The authors acknowledge Ed Lindsey, Jim Hughes, Rick Heredia, and Chuck Heinbockel for their contributions to this work.

VI. References

1. HAAN, S. W. ET al., Design and modeling of ignition targets for the National Ignition Facility. *Physics of Plasmas* **2**, *6*, 2480–7 (1995).

2. AMENDT, P., CERJAN, C., HAMZA, A., HINKEL, D. E., MILOVICH, J. L. AND ROBEY, H. F., Assessing the Prospects for Achieving Double-Shell Ignition on the National Ignition Facility Using Vacuum Hohlraums. *Physics of Plasmas* **14**, 56312 (2007).

3. KYRALA, G. A. et al., Detailed Diagnosis of a Double-Shell Collision under Realistic Implosion Conditions. *Physics of Plasmas* **13**, 56306 (2006).

4. KYRALA, G. A. et al., Direct drive double shell target implosion hydrodynamics on OMEGA. *Laser and Particle Beams* **23**, 187–192 (2005).

5. BONO, M. et al., Fabrication of Double-Shell Targets with a Glass Inner-Capsule. *Fusion Science and Technology* **51**, 611–625 (2007).

6. HIBBARD, R. L., BONO, M. J., AMENDT, P. A., BENNETT, D. W. AND CASTRO, C., Precision Manufacturing of Inertial Confinement Fusion Double Shell Laser Targets for OMEGA. *Fusion Science and Technology* **45**, 117–123 (2004).

7. CANAUD, B., LAFFITE, S. AND TEMPORAL, M., Shock ignition of direct-drive double-shell. *Nuclear Fusion* **51**, 62001 (2011).

8. MILOVICH, J. L., AMENDT, P., MARINAK, M. AND ROBEY, H., Short-Wavelength Perturbation Growth Studies for NIF Double-Shell Ignition Target Designs. *IFSA Conference Proceedings* (2003).

9. ROBEY, H. F. et al., Experimental Measurement of Au M-Band Flux in Indirectly Driven Double-Shell Implosions. *Physics of Plasmas* **12**, 72701 (2005).

10. AMENDT, P. et al., Indirect-Drive Noncryogenic Double-Shell Ignition Targets for the National Ignition Facility: Design and Analysis. *Physics of Plasmas* **9**, 2221 (2002).

11. AMENDT, P., COLVIN, J. D., RAMSHAW, J. D., ROBEY, H. F. AND LANDEN, O. L., Modified Bell – Plesset effect with compressibility: Application to double-shell ignition target designs. *Physics of Plasmas* **10**, *3*, 820–829 (2003).

12. MILOVICH, J. L. et al., Multimode Short-Wavelength Perturbation Growth Studies for NIF Double-Shell Ignition Target Designs. *Physics of Plasmas* **11**, 1552 (2004).

13. VARNUM, W. S. et al., Progress Toward Ignition with Noncryogenic Double-Shell Capsules. *Phys. Rev. Lett.* **84**, *22*, 5153 (2000).

14. MEYER, S. F., Metallic coating of microspheres. *Journal of Vacuum Science and Technology* **18**, 1198–1204 (1981).

15. HENDRICKS, C. D., CRANE, J. K., HSIEH, E. J. AND MEYER, S. F., Metallic and Non-Metallic Coatings for Inertial Confinement Fusion Targets. *Thin Solid Films* **83**, 61–72 (1981).

16. MAYER, A. AND CATLETT, D. S., Plating Discrete Microparticles for Laser-Fusion Targets, *Plating & Surface Finishing* **65**, 42–46 (1978).

17. MAYER, A., Electrolytic Plating Apparatus for Discrete Microsized Particles. U.S. Patent 3994796 (1976).

18. MAYER, A. AND DOTY, W., Advances in Plating discrete hollow glass microspheres. *Technical Digest of the Topical Meeting on Inertial Confinement Fusion,* THB23 (1980).

19. ILLIGE, J. D., YU, C. M. AND LETTS, S. A., Metal coatings for laser fusion targets by electroplating. *Journal of Vacuum Science and Technology* **18**, *3*, 1209–1213 (1981).

20. YU, C. M. AND ILLIGE, J. D., Apparatus for Electroplating Particles of Small Dimension. U.S. Patent 4316786, (1982).

21. JANKOWSKI, A. F., SAW, C. K., HARPER, J. F., VALLIER, B. F., FERREIRA, J. L. AND HAYES, J. P., Nanocrystalline growth and grain-size effects in Au-Cu electrodeposits. *Thin Solid Films* **494**, 268–273 (2006).

22. JANKOWSKI, A. F., SAW, C. K. AND HAYES, J. P., The thermal stability of nanocrystalline Au – Cu alloys. *Thin Solid Films* **515**, 1152–1156 (2006).

23. WANG, Y. M., JANKOWSKI, A. F. AND HAMZA, A. V., Strength and thermal stability of nanocrystalline gold alloys. *Scripta Materialia* **57**, 301–304 (2007).

24. BRUN, E. et al. Influence of the Electrochemical Parameters on the Properties of Electroplated Au-Cu Alloys. *Journal of The Electrochemical Society* **158**, *4*, D223 (2011).

25. DURUT, F. et al., Phenomenological model for gold-copper electrodeposition: application to thick coatings, F. Durut. *Fusion Science and Technology* **70**, *2*, 341–50 (2016).

26. BOTREL, R. AND BOURCIER, H., Surface Treatment Electrode. U.S. Patent 8246797 (2012).

27. BUNN, T., HORWOOD, C. AND STADERMANN, M., Cathode System for Electrodeposition of Metals on Microspheres. US Patent 62522746, (2017).